



HAL
open science

Minc00344 and Mj-NULG1a effectors interact with GmHub10 protein to promote the soybean parasitism by *Meloidogyne incognita* and *M. javanica*

Reneida Aparecida Godinho Mendes, Marcos Fernando Basso, Janaina Fernandes de Araújo, Bruno Paes de Melo, Rayane Nunes Lima, Thuane Pires Ribeiro, Vanessa da Silva Mattos, Erika Valéria Saliba Albuquerque, Maira Grossi-De-Sa, Suelen Nogueira Dessaune Tameirao, et al.

► **To cite this version:**

Reneida Aparecida Godinho Mendes, Marcos Fernando Basso, Janaina Fernandes de Araújo, Bruno Paes de Melo, Rayane Nunes Lima, et al.. Minc00344 and Mj-NULG1a effectors interact with GmHub10 protein to promote the soybean parasitism by *Meloidogyne incognita* and *M. javanica*. *Experimental Parasitology*, 2021, 229, 10.1016/j.exppara.2021.108153 . hal-03435690

HAL Id: hal-03435690

<https://hal.science/hal-03435690>

Submitted on 14 Oct 2022

HAL is a multi-disciplinary open access archive for the deposit and dissemination of scientific research documents, whether they are published or not. The documents may come from teaching and research institutions in France or abroad, or from public or private research centers.

L'archive ouverte pluridisciplinaire **HAL**, est destinée au dépôt et à la diffusion de documents scientifiques de niveau recherche, publiés ou non, émanant des établissements d'enseignement et de recherche français ou étrangers, des laboratoires publics ou privés.



Minc00344 and Mj-NULG1a effectors interact with GmHub10 protein to promote the soybean parasitism by *Meloidogyne incognita* and *M. javanica*

Reneida Aparecida Godinho Mendes^{a,b,1}, Marcos Fernando Basso^{a,h,1},
Janaina Fernandes de Araújo^a, Bruno Paes de Melo^{a,c}, Rayane Nunes Lima^a,
Thuane Pires Ribeiro^a, Vanessa da Silva Mattos^a, Erika Valéria Saliba Albuquerque^a,
Maira Grossi-de-Sa^{a,d}, Suelen Nogueira Dessaune Tameirao^e, Rodrigo da Rocha Fragoso^e,
Maria Cristina Mattar da Silva^{a,h}, Florence Vignols^f, Diana Fernandez^{a,d,h},
Maria Fatima Grossi-de-Sa^{a,g,h,*}

^a Embrapa Genetic Resources and Biotechnology, Brasília-DF, 70297-400, Brazil

^b Federal University of Brasília, Brasília-DF, 70910-900, Brazil

^c Federal University of Viçosa, Viçosa-MG, 36570-900, Brazil

^d IRD, Cirad, Univ Montpellier, IPME, 911, Avenue Agropolis, 34394, Montpellier Cedex 5, France

^e Embrapa Cerrados, Planaltina-DF, 73310-970, Brazil

^f Biochimie et Physiologie Moléculaire des Plantes, CNRS/INRA/Université de Montpellier/SupAgro, Montpellier, France

^g Catholic University of Brasília, Brasília-DF, 71966-700, Brazil

^h National Institute of Science and Technology-INCT PlantStress Biotech-EMBRAPA, Brazil

ARTICLE INFO

Keywords:

Plant-parasitic nematodes
Effector
RNA interference
Protein-protein interaction
Nematode management

ABSTRACT

Several economically important crops are susceptible to root-knot nematode (RKNs). *Meloidogyne incognita* and *M. javanica* are the two most reported species from the RKN complex, causing damage to several crops worldwide. The successful outcome of the *Meloidogyne*-plant interaction is associated with molecular factors secreted by the nematode to suppress the plant's immune response and promote nematode parasitism. In contrast, several plant factors are associated with defense against nematode infection. In this study, we identified and characterized the specific interaction of Minc00344 and Mj-NULG1a effectors with soybean GmHub10 (*Glyma.19G008200*) protein *in vitro* and *in vivo*. An *Arabidopsis thaliana* T-DNA mutant of *AtHub10* (*AT3G27960*, an orthologous gene of *GmHub10*) showed higher susceptibility to *M. incognita*. Thus, since soybean and *A. thaliana* Hub10 proteins are involved in pollen tube growth and indirect activation of the defense response, our data suggest that effector-Hub10 interactions could be associated with an increase in plant susceptibility. These findings indicate the potential of these effector proteins to develop new biotechnological tools based on RNA interference and the overexpression of engineered Hub10 proteins for the efficient management of RKN in crops.

1. Introduction

Plant-parasitic nematodes (PPNs) are among the major agricultural parasites causing annually significant economic losses worldwide (Bernard et al., 2017). PPNS disturb plant roots by altering the cell cycle, increasing the size of parasitized cells, and causing cell hyperproliferation and the development of nematode feeding sites (de Almeida Engler et al. 2004, 2012, 2015; de Souza Junior et al., 2017;

Shukla et al., 2018). These disorders disrupt water and nutrient uptake and reduce plant growth and yield (Melakeberhan et al., 1987; Carneiro et al., 2002; Lu et al., 2014). Root-knot nematode (RKN) are obligate sedentary endoparasites from the genus *Meloidogyne* spp. (Trudgill and Blok 2001). Among the RKNs, *Meloidogyne incognita* and *M. javanica* are the two major species most commonly reported to cause damage in several plant cultures of economic importance worldwide (Abad et al., 2008). The life cycle of these species comprises six stages, namely, egg,

* Corresponding author. Embrapa Genetic Resources and Biotechnology, PqEB Final, W5 Norte, PO Box 02372, 70770-901, Brasília-DF, Brazil.

E-mail address: fatima.grossi@embrapa.br (M.F. Grossi-de-Sa).

¹ These authors contributed equally to this study.

J1 (first-stage juvenile), J2 (second-stage juvenile), J3 (third-stage juvenile), J4 (fourth-stage juvenile), and adults (female and male) (Triantaphyllou and Hirschmann 1960). J3, J4, and females are sedentary endophytes, while eggs, J1, and preparasitic J2 are exophytes for the majority of *Meloidogyne* species (Abad et al., 2008; Castagnone-Sereno et al., 2013).

Meloidogyne-host plant interactions include an extensive molecular immunity network involved in defense and counterdefense (Lin et al., 2013; Gillet et al., 2017). Regarding basal defense, after recognition of nematode elicitors, host plants increase the production of reactive oxygen and nitrogen species (e.g., hydrogen peroxide) and other toxic compounds derived from secondary metabolism (Melillo et al., 2011; Holscher et al., 2014; Manosalva et al., 2015; Kong et al., 2015; Silva et al., 2018). In contrast, *Meloidogyne* spp. increase the production and release of antioxidant and detoxifying compounds (e.g., ROS scavengers, glutathione peroxidases, peroxidases, peroxiredoxins, and catalases) (Bellafiore et al., 2008; Dubreuil et al., 2011; Shinya et al., 2013; Basso et al., 2020b), and effector proteins to overcome host defenses (Xie et al., 2016; Lin et al., 2016; Bournaud et al., 2018). Thus, for successful infection, nematodes seek to minimize plant cell damage and depend on living cells to develop a feeding site and promote their reproductive cycle in host plants (Gheysen and Mitchum 2011; Goverse and Smant 2014). For this purpose, several nematode effector proteins attempt to manipulate different biological processes (e.g., neutralize the host oxidative pathway or suppress programmed cell death) and defense responses (e.g., plant immune system) of the plants (Xie et al., 2016; Nguyen et al., 2018; Bournaud et al., 2018; Shi et al., 2018; Grossi-de-Sa et al., 2019; Zhao et al., 2019). For example, Mi-MSP18 (Grossi-de-Sa et al., 2019) and Mi-Msp40 (Niu et al., 2016) effectors were demonstrated to act in cell death suppression and can enhance plant susceptibility and modulate host immunity. Similarly, the Mi-MiPM effector interacts with subunit 5 of the COP9 signalosome (CSN5), but the biological consequences of this interaction have not been determined (Bournaud et al., 2018). Likewise, the Mi-Mi8D05 effector interacts with plant aquaporin tonoplast intrinsic protein 2 (TIP2), suggesting that it regulates solute and water transport within giant cells to promote the parasitic interaction (Xue et al., 2013). Other examples include Mi-MiPFN3, which disrupts the plant actin cytoskeleton to promote giant cell formation (Leelarasamee et al., 2018), and Mi-MiMIFs promote parasitism by interfering with annexin-mediated plant immune responses (Zhao et al., 2019).

Secretome analyses from the *Meloidogyne* genus enabled the identification of numerous candidate effector proteins (Huang et al., 2003; Bellafiore et al., 2008; Rutter et al., 2014). For example, Minc00344 and Mj-NULG1a attracted our attention. The Minc00344 also showed specific expression in the subventral gland (SvG) and was strongly upregulated during the first three parasitic time points studied (3, 7, and 14 days post-inoculation; dpi). This effector belongs to the MAP-1 gene family, which is a candidate *M. incognita* avirulence protein (Castagnone-Sereno et al., 2009; Tomalova et al., 2012). Similarly, the *M. javanica* Mj-NULG1a effector is upregulated in parasitic J2s and declines in later parasitic stages. The Mj-NULG1a encoded a protein was predicted with two nuclear localization signals and colocalized in giant cells' nuclei (Lin et al., 2013). Although this protein does not have a defined biological function, it was suggested to act as an effector protein during plant parasitism (Danchin et al., 2013).

Although several *M. incognita* and *M. javanica* effectors have already been identified, little is known about their targets or action mechanisms when secreted in the plant (Mejias et al., 2019; Vieira and Gleason 2019). Previous studies from protein-protein interactions between *A. thaliana* and phytopathogens (bacteria, oomycetes, and fungi) showed that several effector proteins from different pathogens interact preferentially with 15 hub proteins of the host plant (Mukhtar et al., 2011; Consortium 2011; Wessling et al., 2014). Among these 15 *A. thaliana* hub proteins, *AtHub10* (AT3G27960) is targeted by six effectors from *Pseudomonas syringae* and *Hyaloperonospora arabidopsidis*

(Mukhtar et al., 2011; Wessling et al., 2014). *AtHub10* is a kinesin light chain-related protein 2 (KLCR2) that acts as a microtubule-associated motor protein that moves cargo along microtubule filaments and plays a crucial role in various plant processes, including pollen tube growth, and is associated with plant defense activation (Reddy and Day 2001; Li et al., 2019). Kinesin light chain (KLC) proteins utilize their tetrapeptide repeat (TPR) domain to interact with several different cargos, while KLC1 and KLC2 kinesin isoforms exhibit differential binding properties for those cargos (Burstenbinder et al., 2013; Abel et al., 2013). The TPR domain is found in a wide range of proteins and is arranged in tandem with until 16 TPR units, which mediate the assembly of multiprotein complexes, such as anaphase-promoting complex (APCs) subunits, cell division control (CDCs), cyclin-dependent kinases (CDKs), among other (Das et al., 1998). All TPR-containing proteins are closely related to the cell cycle control, in which APC, CDC, and CDKs are directly involved, while KLC proteins are also involved in this process, but in a second level (Reddy and Day 2001; Li et al., 2019). Notably, a common feature among these TPR-containing proteins is directly or indirectly part of the commonly known mechanism as "growth-defense trade-off" (Huot et al., 2014). In other words, the modulation of the cell cycle (to growth and development) versus the cellular immune system (to defense or counter-defense) are strongly related, and the disturbance of one of these mechanisms (either by biotic or abiotic stresses) requires the reprogramming of the priorities of the plant in this adverse moment in order to overcome (achieve resistance or tolerance) these unexpected events. At the same time, we know that a vast majority, if not all pathogens (sure including nematodes), directly or indirectly interfere with the cell cycle or host plants' immune system. Given these previous findings, the role of KLC proteins in the growth and defense mechanism becomes a little more evident for us. However, information about the role of KLCR2, or more specifically, *Hub10* proteins, is still quite limited in plant-nematode interaction.

Curiously, overaccumulation of tomato kinesin-like protein (MG565981) was associated with improved plant resistance to *Tobacco mosaic virus* infection. However, its role during the viral infection has not been elucidated to date (Abdelkhalik et al., 2019). Additionally, there is no information showing the interaction of nematode effectors with plant kinesin proteins and the consequences of this interaction on plant resistance to nematode infection.

Soybean (*Glycine max*) is one of the most important agricultural commodities worldwide (Hartman et al., 2011; USDA 2020). The main soybean cultivars are considered to be highly susceptible to RKN, and associated with inefficient nematode management; significant yield penalties and economic losses are also constantly reported in diseased crops (Mazzetti et al., 2019). Thus, a better understanding of the soybean-nematode molecular interaction may enable the development of new biotechnological tools (NBTs) that contribute to the management and control of the nematodes in this culture (Basso et al. 2019, 2020a). This study validated the specific interaction between Minc00344 and Mj-NULG1a effectors with the soybean *GmHub10* (*Glyma.19G008200*) protein orthologous to *AtHub10* using *in vitro* and *in vivo* approaches. Curiously, using an *A. thaliana* T-DNA mutant of the *AtHub10* gene, our data suggested that disruption of *AtHub10* protein function can be associated with an increase in plant susceptibility. The collective findings of this study suggest that the interactions among Minc00344, Mj-NULG1a, and *GmHub10* proteins can be essential to manipulate the host plant (plant or giant cell developmental and defense pathways) and promote RKN parasitism.

2. Materials and methods

2.1. *In silico* analysis of the effectors Minc00344 and Mj-NULG1a, and soybean *GmHub10* network

All sequences and features of *M. incognita* and *M. javanica* genes were retrieved from BioProject ID PRJEB8714 (samples: ERS1696677 and

ERS671129, respectively) (Blanc-Mathieu et al., 2017) from the online WormBase Parasite Database version WBPS13 (Lee et al., 2017). Conserved domains were identified using the CDD Database from NCBI (Marchler-Bauer et al., 2015). Pairwise identity matrices were generated using Sequence Demarcation Tool Version 1.2 software (Muhire et al., 2014). Phylogenetic analyses from effector sequences were performed using the Phylogeny.fr web service (Dereeper et al., 2008). For this, sequences were aligned with MUSCLE software (Edgar 2004), and the alignment was curated by the Gblocks model. Then, phylogenetic analyses were performed using the maximum likelihood method with PhyML software using the approximate likelihood-ratio test (aLRT) SH-like branch support and GTR and WAG substitution models for nucleotide and amino acid sequences, respectively. Phylogeny trees were generated and visualized by TreeDyn software, which was implemented in this same web service.

Sequences and features from soybean genes were retrieved from *Glycine max Wm82.a2.v1* (BioProject: PRJNA19861) (Schmutz et al., 2010) by the Phytozome v.12 database (Goodstein et al., 2012). Conserved domains in the gene sequences were identified using the CDD Database from NCBI (Marchler-Bauer et al., 2015), annotation confirmed by the HMMER prediction server (Wheeler and Eddy 2013), and nuclear signal localization (NLS) motifs were predicted using the NLSstradamus online tool (Nguyen Ba et al., 2009). The pairwise identity matrices and phylogenetic analyses were performed as described above. The interactome network from soybean and *A. thaliana* Hub10 proteins with their interactor proteins was retrieved from platform STRING database v.11 (Szklarczyk et al., 2019). The organ- and tissue-specific expression of the soybean genes were presented by the heat map plot created by the PhytoMine tool (<https://phytozome.jgi.doe.gov/phytomine/begin.do>) using all gene expression data in the database regarding tissue- and organ-specific expression.

2.2. *M. incognita* J2 inoculum

The *M. incognita* J2 race 1 and race 3 were obtained from tomato plants (*Solanum lycopersicum* cv. Santa Clara) inoculated and maintained for eight to ten weeks under greenhouse conditions. Infected roots were washed and macerated using a blender after treatment with 0.5% sodium hypochlorite. Eggs were harvested, rinsed with tap water, and subsequently separated from root debris using 100- to 550- μ m sieves (Hussey and Barker 1973). Then, the eggs were hatched under aerobic conditions at 28 °C, and J2 were harvested every two days, decanted and quantified under a microscope using counting chambers.

2.3. *In vitro* and *in vivo* transactivation assays for the protein-protein interaction evaluation and gene expression assays

The protein-protein interaction was performed to evaluate the interaction of the Minc0344 and Mj-NULG1a (GenBank ID: JN836601) effectors with soybean GmHub4 (COP9 signalosome complex subunit 5, CSN5, *Glyma.06G076000*; AtHub4, *AT1G22920*), GmHub6 (TCP family transcription factor, *Glyma.17G099100*; AtHub6, *AT3G47620*), GmHub10 (Kinesin light chain, *Glyma.19G008200*; AtHub10, *AT3G27960*), GmHub12 (APC8/Anaphase promoting complex subunit, *Glyma.11G026400*; AtHub12, *AT3G48150*), GmHub17 (TCP family transcription factor, *Glyma.02G105900*; AtHub16, *AT1G69690*), GmHub42 (Transcription factor UNE12-Related, *Glyma.19G160900*; AtHub22, *AT4G02590*), GmHub47 (Jasmonate ZIM domain-containing protein, *Glyma.09G174200*; AtHub24, *AT3G17860*), and GmHub61 (Uncharacterized conserved protein containing an emsy amine-terminus domain, *Glyma.02G178800*; AtHub25, *AT5G06780*). Soybean hubs sequences were isolated from cDNA of the soybean root cv. Williams 82, cloned into pGEMT easy vector (Promega, Madison, Wisconsin, USA), sequenced and subcloned into the entry vector with gateway cloning system (pENTR11; Invitrogen) and pGADT7-AD and pGBKT7-BD destination vectors. Sequence identities were confirmed by comparison with

gene sequences retrieved from *Glycine max Wm82.a2.v1* (BioProject: PRJNA19861) (Schmutz et al., 2010) by the Phytozome v.12 database (Goodstein et al., 2012). The full-length cDNA sequences from Minc00344 and Mj-NULG1a effectors were synthesized by the company Epoch Life Science (Sugar Land, TX, EUA), cloned in pENTR11 vector, propagated in *E. coli* DH5 α , and subsequently transferred to pGADT7-AD and pGBKT7-BD destination vectors using Gateway™ LR Clonase™ Enzyme mix (Thermo Fisher Scientific, Waltham, Massachusetts, USA). Y2H experiments were performed using the Matchmaker™ GAL4 Two-Hybrid System 3 (Clontech, Mountain View, CA, USA) based on GAL4 binding (BD) and transactivation (AD) domains present in these destination vectors. Both Y2H vectors were sequentially co-transformed into the competent cells of *Saccharomyces cerevisiae* strain YRG2 (Matu, ura3-52, his3-200, ade2-101, lys2-801, trp1-901, leu2-3, 112, gal4-542, gal80-538) using the lithium acetate/polyethylene glycol (PEG) method. Single colonies from co-transformed yeasts were grown overnight in a selective yeast nitrogen base (YNB) medium in a shaking incubator at 180 rpm and 28 °C. Yeast cells were diluted in fresh YNB medium to an optical dilution (OD₆₀₀) of about 1 to 0.01. Then, 100 μ l of suspension was plated onto a synthetic dropout medium lacking leucine, tryptophan, and histidine, containing 5 to 10 mM 3-amino-1,2,4-triazole (3-AT) *His3* gene-product competitive inhibitor, and incubated at 28 °C for three to five days. The empty pGADT7-AD and pGBKT7-BD vectors were used as negative controls of protein-protein interaction, while pGADT7-AD::NIG and pGBKT7-BD::AtWWP1 were used as positive controls. The *A. thaliana* AtWWP1 (*AT2G41020*) and NIG (*AT4G13350*) protein interactions were previously shown by Calil et al. (2018).

BiFC assays were performed using different combinations of the *A. tumefaciens* strain GV3101 carrying the binary vectors pSITE BiFC cEFYF (GU734652) and nEYFP (GU734651) containing the 35S:GmHub10-cYFP and 35S:Minc00344-nYFP or 35S:Mj-NULG1a-nYFP fusion proteins. The *A. tumefaciens* co-culture was co-infiltrated into the abaxial surface of *N. tabacum* leaves at an OD₆₀₀ nm 0.7 in a final ratio of 1:1. The yellow fluorescence was analyzed in the epidermal cells three days after infiltration using a Zeiss inverted LSM510 META laser scanning microscope equipped with an argon laser and a helium laser as excitation sources. The yellow fluorescent protein (YFP) was excited at 514 nm using the argon laser, and YFP emission was detected using a 560-615-nm filter.

2.4. *GmHub10* expression profile during *M. incognita* infection

Soybean conventional genotype PI595099 (nematode-resistant) and cultivar BRS133 (nematode-susceptible) considered contrasting for the RKN resistance (Beneventi et al., 2013) were inoculated with 1,000 *M. incognita* J2 race 1, and root samples were harvested at 3, 8, 15, and 25 dpi from mock and nematode inoculated plants. Total RNA was purified using Concert™ Plant RNA Reagent (Invitrogen, Carlsbad, CA, USA) supplemented with PVP-40. The RNA concentration was estimated using a spectrophotometer (NanoDrop 2000, Thermo Scientific, Waltham, Massachusetts, USA) and integrity was evaluated with 1% agarose gel electrophoresis. RNA samples were treated with RNase-free RQ1 DNase I (Promega, Madison, Wisconsin, USA) according to the manufacturer's instructions. Then, 2 μ g of DNase-treated RNA was used as a template for cDNA synthesis using Oligo-(dT)₂₀ primer and SuperScript III RT (Life Technologies, Carlsbad, CA, USA), according to the manufacturer's instructions. The cDNA was quantified by spectrophotometry and diluted with nuclease-free water to 200 ng/ μ l. RT-PCR assays were performed in an Applied Biosystems 7500 Fast Real-Time PCR System (Applied Biosystems, Foster City, CA, USA) using 400 ng of cDNA, 0.2 μ M of each gene-specific primer and GoTaq® qPCR Master Mix (Promega, Madison, Wisconsin, USA). The conditions for RT-PCR included an initial 95 °C for 10 min, then 40 cycles of 95 °C for 15 s and 60 °C for 1 min, followed by a final melting curve analysis. The expression profile of the *GmHub10* gene during nematode infection was measured by RT-PCR

using specific primers and normalized with *GmCYP18* (*Glyma.12G024700*) as an endogenous reference gene (Supplementary Table 1). The thermocycling reactions and conditions used are the same as described above. Four biological replicates were used for each treatment, while each biological replicate was composed of four plants. All cDNA samples were carried out in technical triplicate, while primer efficiencies and target-specific amplification were confirmed by a single and distinct peak in the melting curve analysis. The relative expression level was calculated using the $2^{-\Delta CT}$ method (Schmittgen and Livak 2008).

2.5. Resistance assessment of the *A. thaliana* AtHub10 mutant to the *M. incognita*

The *A. thaliana* seeds from the mutant (T-DNA insertion; SALK mutant: SALK_142719) line for the *AtHub10* gene (*AT3G27960*, an orthologous gene of the soybean *GmHub10*; Suppl. File S2) and null mutant line to the *Enhanced disease susceptibility 1* (*Eds1*; *AT3G48090*; SALK mutant: SALK_034340) gene were obtained from the Arabidopsis Biological Resource Center (ABRC; Columbus OH, 43210, USA). *A. thaliana* seeds were surfaced sterilized and sown on selective (kanamycin) Murashige and Skoog (MS)-containing agar plates. Plates were stratified in the dark at 4 °C for 72 h. Plants were grown in a growth chamber at 22 °C under 12h light/12 h dark photoperiod. Plants *in vitro* kanamycin-resistant were transferred for *in vivo* condition into the substrate: sand (autoclaved commercial substrate and sand in 1:1 proportion) and grown as described above. Transgenic plants from *AtEds1* and *AtHub10* lines were confirmed for NPTII (neomycin-phosphotransferase II) protein accumulation by serological assays using the ELISA assay with Agdia kit (Agdia Patho Screen nptII). Then, transgenic and wild-type seedlings (two or three-week-old plants) were inoculated with 250 *M. incognita* J2 as described above. Inoculated roots were harvested at 5, 10, 15, and 25 dpi, stained with acid fuchsin as described by Byrd et al. (1983), and the penetration efficiency in the root and the post-penetration development of the nematode, and the formation of the galls were evaluated. In addition, the number of eggs per gram of root,

the number of J2 per gram of root, the number of galls per gram of root, and NRF were determined from an additional plant set at 40 dpi. The NRF was determined with Oostenbrink’s formula: $RF = \text{final J2 number} / \text{initial J2 number}$ or $\text{nematode final population} / \text{initial population}$ (Oostenbrink 1966; Windham and Williams 1987). The *AtEds1* mutant line was used as a susceptibility control (Parker et al., 1996; Cui et al., 2017). Each *A. thaliana* line was composed of 14 to 20 plants, which were divided into three biological replicates.

3. Results

3.1. In silico analysis of Meloidogyne effectors

Pairwise comparisons of amino acid sequences showed that Minc00344 and Mj-NULG1a have low sequence identity with each other, ranging from 10 to 30% (Fig. 1A). Additionally, compared to other proteins produced in nematode-secretory organs, either predicted or validated to be involved in plant parasitism, the percentage of identities observed ranged from 12 to 92%. Phylogenetic analysis also showed that these two effectors studied here are grouped separately, originating from two well-defined groups (Fig. 1B). All these collective data from *in silico* analysis indicated that these two *Meloidogyne* effectors are distant at the sequence and phylogenetic levels but are closely associated with plant parasitism.

3.2. Protein-protein interaction between Minc00344 and Mj-NULG1a effectors with soybean GmHub10 protein

Previous interactome studies developed with *A. thaliana* and different phytopathogens as a model identified some plant hub proteins that are targeted by several effectors during the plant-pathogen interaction. In this study, eight of these hub proteins were chosen for evaluating the interaction with Minc00344 and Mj-NULG1a effectors. To this end, the orthologous genes of these *A. thaliana* hub proteins were searched in the soybean transcriptome, and the corresponding CDS sequence was cloned into the destination vector for *in vitro* and *in vivo*

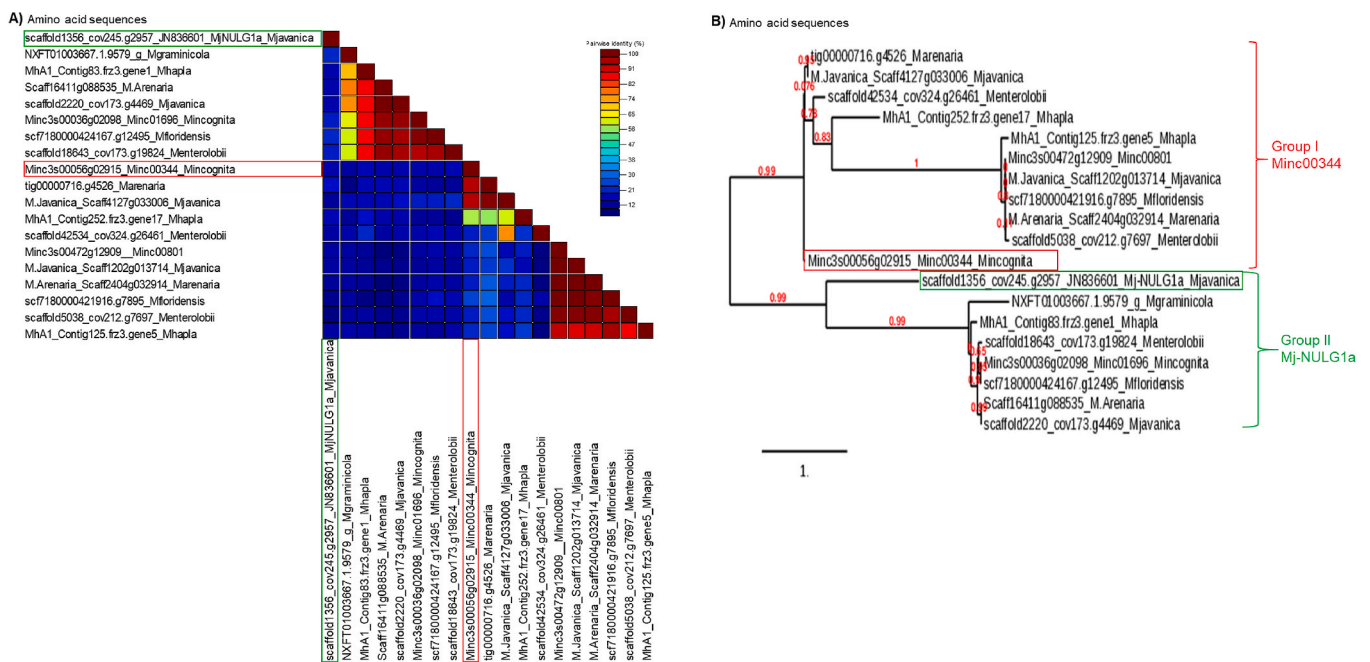


Fig. 1. In silico analysis of the nematode effector protein sequences. (A) Pairwise sequence identity matrices of amino acid sequences generated using Sequence Delineation Tool version 1.2 software. (B) Evolutionary analysis of amino acid sequences generated by the Phylogeny.fr web service. Highlighted in the red and green box are, respectively, the *M. incognita* and *M. javanica* effector proteins studied in this work. Gene sequences were retrieved from the online WormBase Parasite Database version WBPS13.

protein-protein interaction assays. Yeast two-hybrid (Y2H) assays were performed with all these proteins, but protein-protein interactions were observed only between Minc00344 and Mj-NULG1a with soybean GmHub10 protein (Fig. 2A; Supplementary Fig. 1A and B). The Minc00344 effector showed specific interaction with the GmHub10 protein both in Y2H (Fig. 2B and C) and *in planta* by bimolecular fluorescence complementation (BiFC) assays (Fig. 2D). Similarly, the Mj-NULG1a effector also showed specific interaction with the GmHub10

protein in both Y2H (Fig. 2E) and BiFC assays (Fig. 2F). In addition, Mj-NULG1a and GmHub10 proteins were considered to have a stronger interaction than Minc00344-GmHub10 based on the 3AT competitive inhibitor added to the selective medium (Fig. 2C and E). In the same sense, both Minc00344 and Mj-NULG1a effector proteins were unable to autoactivate in Y2H assays (Fig. 2B and E), while GmHub10 showed autoactivation potential (Fig. 2B). Also, we discard the possibility of self-assembly of nYFP and cYFP, resulting in non-genuine fluorescence from

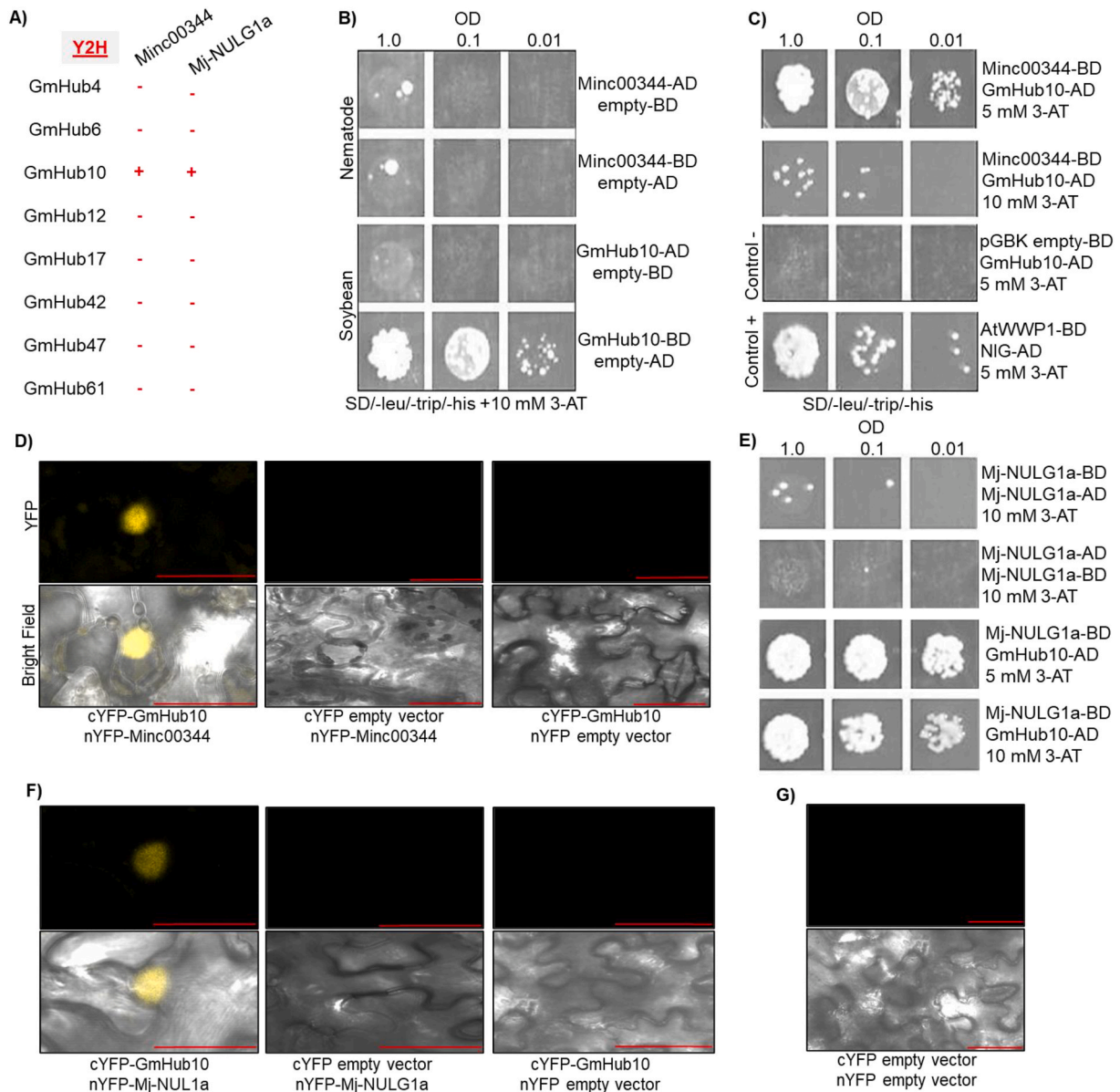


Fig. 2. Protein-protein interaction assays between the Minc00344 and Mj-NULG1a effectors with eight soybean GmHub proteins. (A) Yeast two-hybrid (Y2H) results for the Minc00344 and Mj-NULG1a effectors and the soybean GmHub4 (*Glyma.06G076000*), GmHub6 (*Glyma.17G099100*), GmHub10 (*Glyma.19G008200*), GmHub12 (*Glyma.11G026400*), GmHub17 (*Glyma.02G105900*), GmHub42 (*Glyma.19G160900*), GmHub47 (*Glyma.09G174200*), and GmHub61 (*Glyma.02G178800*). For interaction assays between effector-GmHub10 proteins, Minc00344 and Mj-NULG1a proteins were expressed in yeast cells fused in the GAL4 binding domain (BD), while GmHub10 protein was expressed in yeast cells fused in the GAL4 activation domain (AD). The interactions between these proteins were examined by monitoring histidine prototrophy. Yeast cells were transformed with a combination of DNA constructs and proteins were expressed in yeast and assayed for interaction on selective synthetic medium (SD) in the presence of 5–10 mM 3-amino-1,2,4-triazol (3-AT) and cell dilutions at an optical density (OD) of 1.0, 0.1 or 0.01. (B) Autoactivation assays with Minc00344 and GmHub10 proteins. (C) Minc00344 and GmHub10 protein interactions in Y2H screening. The protein-protein interactions were evaluated using pGBK empty vector-BD + GmHub10-AD and AtWWP1 (*AT2G41020*)-BD + NIG (*AT4G13350*)-AD as negative and positive controls, respectively. (D) *In planta* interaction between Minc00344 and GmHub10 by BiFC assays. The fluorescence (yellow fluorescent protein; YFP) images were acquired using *N. tabacum* leaves co-expressing the binary vectors pSITE BiFC cYFP (GU734652) and nYFP (GU734651) with the 35S:GmHub10-cYFP + 35S:Minc00344-nYFP fusion proteins. (E) Autoactivation assays and protein-protein interaction using Y2H screening with Mj-NULG1a and GmHub10 proteins. (F) *In planta* interaction between Mj-NULG1a and GmHub10 by BiFC assays performed in *N. tabacum* leaves. (G) Negative control based on empty vectors used in BiFC assays. They are representative samples from three independent biological repeats. Scale bars, 20 μ m.

target proteins interaction. Furthermore, a regular pattern of GFP or YFP fluorescence resulting from self-assembly allows fluorescence visualization both in cytoplasm and nuclei in a diffuse way. In our fluorescent fields, we only observed fluorescence in nuclei. Considering that AtHub10 and GmHub10 proteins are transcription factors and encompasses a nuclear localization signal, we can consider the fluorescence genuine and resulting from Hub10-effector interaction. In the face of these facts, these data showed that although these two effectors Minc00344 and Mj-NULG1a are from different nematode species, they can interact with the same host protein.

3.3. In silico characterization of the GmHub10 network sequences

GmHub10 and its homolog gene (*Glyma.05G007800*) showed higher amino acid identity with *AtHub10* (approx. 70%), while lower sequence identity (approx. 20%) was observed with seven other soybean GmHub proteins (Fig. 3A). In addition, phylogenetic analysis using amino acid sequences showed that *GmHub10* and its homologous gene are grouped closer to *AtHub10* (Fig. 3B). The biological function of GmHub10 is implicated in pollen tube growth and regulation of the defense response, and its protein contains several tetratricopeptide repeat domains (pfam13424) and nuclear localization signals (Table 1). The protein-protein interaction network retrieved from the STRING database highlighted that GmHub10 is the core protein that interacts with the other ten proteins (Supplementary Fig. 2A), similar to the *AtHub10* network (Supplementary Fig. 2B), thereby justifying the designation “Hub protein”. Among these proteins from the *GmHub10* network are kinases, phosphoproteins, Fc2 pre-rRNA processing, zinc finger (Ran-binding) protein, early growth response protein-related, and anaphase-promoting

complex subunit 4 (Table 1). Curiously, the *GmHub10* transcript showed accumulation in all soybean tissues and different conditions with lower accumulation in nodules under symbiotic conditions and roots under ammonia treatment and higher abundance in stems, roots, and pods (Supplementary Fig. 2C). In addition, *GmHub10* showed a positive correlation at gene expression levels in these same different soybean tissues or conditions with all ten major interactor proteins from its network, except for *Glyma.14g125900*, *Glyma.14G125600*, and *Glyma.20G012700* (Supplementary Fig. 2D).

3.4. GmHub10 expression profile in soybean roots during *M. incognita* infection

RT-PCR assays showed that the *GmHub10* gene was not modulated in axillary roots by the nematode infection in either the nematode-resistant genotype PI595099 or the nematode-susceptible cultivar BRS133 (Fig. 3C). However, *GmHub10* gene expression was higher at 3 dpi in the resistant cultivar's roots both in mock or inoculated compared with the susceptible plants. Concerning *GmHub10* gene expression in the four developmental stages (stages I to IV) of the soybean plants, the expression level was only significantly higher at stage I (3 dpi) in the resistant cultivar. In contrast, in the susceptible cultivar, the expression was stable along all four stages.

3.5. Developmental phenotype and resistance assessment of the *A. thaliana* AtHub10 mutant

The *A. thaliana* AtHub10 mutant noninoculated plants showed significative abnormal formation of the nodes and axillary flowers of the

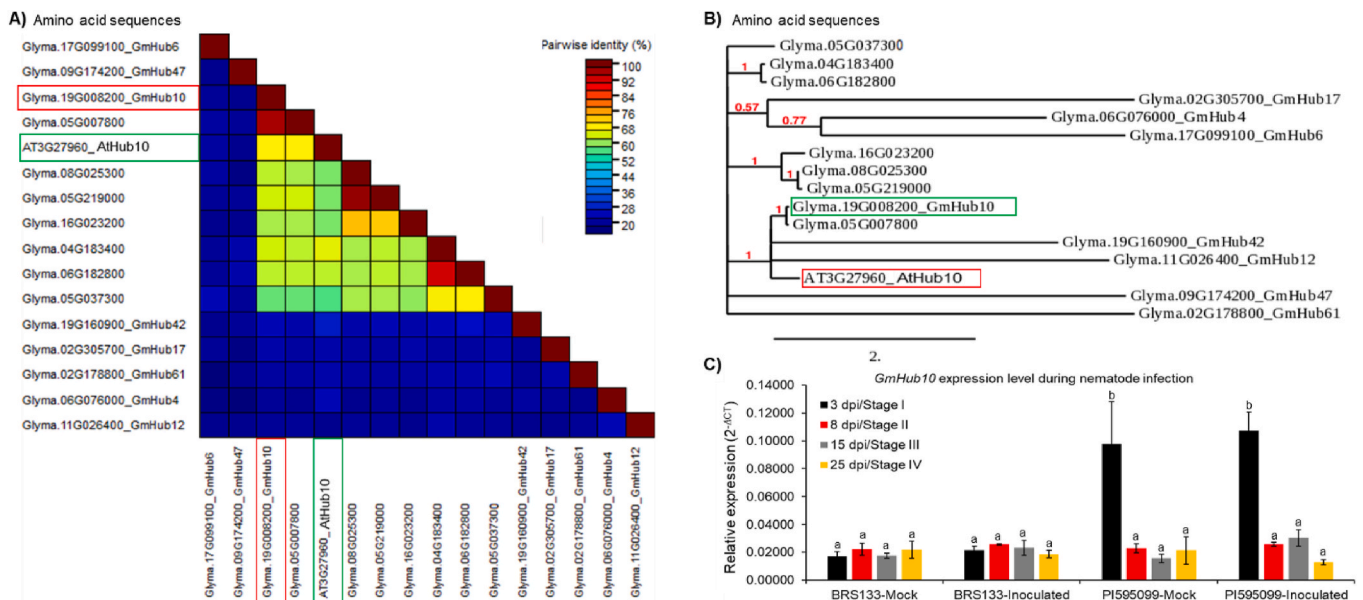


Fig. 3. In silico sequence analysis, expression profile in roots of the soybean plant in different development stages and during *M. incognita* infection of the soybean *GmHub10* (*Glyma.19G008200*) gene. (A) Pairwise sequence identity matrices of amino acid sequences generated using Sequence Demarcation Tool version 1.2 software. In addition, were added in this sequence analysis the GmHub4 (*Glyma.06G076000*), GmHub6 (*Glyma.17G099100*), GmHub12 (*Glyma.11G026400*), GmHub17 (*Glyma.02G105900*), GmHub42 (*Glyma.19G160900*), GmHub47 (*Glyma.09G174200*), GmHub61 (*Glyma.02G178800*) and another seven putative homolog proteins of the GmHub10. (B) Evolutionary analysis from amino acid sequences generated by the Phylogeny.fr web service. Highlighted in the red and green box are, respectively, the GmHub10 and AtHub10 proteins studied in this work. Gene sequences were retrieved from *Glycine max* Wm82.a2.v1 (BioProject: PRJNA19861) by the Phytozome v.12 database. (C) Expression profile of the *GmHub10* gene in roots of the soybean conventional cultivar BRS133 (susceptible) and genotype PI595099 (resistant) considered contrasting for the root-knot nematodes resistance/susceptibility. The expression profile was measured using the RT-PCR assays from mock and *M. incognita* race 3 inoculated plants at 3, 8, 15, and 25 days post-inoculation (dpi). The 3, 8, 15, and 25 dpi corresponding to the development stages I (opening of the second trifoliolate), stages II (opening of the fourth trifoliolate), stages III (opening of the sixth trifoliolate in the cultivar BRS133 and beginning of flowering in the genotype PI595099), and stages IV (beginning of flowering in the cultivar BRS133 and grains boot stage in the genotype PI595099) of the plants maintained in greenhouse conditions. The relative expression values were calculated using the 2^{-ΔCT} formula with the *GmCYP18* gene as an endogenous reference gene (Supplemental Table 1). Error bars represent confidence intervals corresponding to four biological replicates (each biological replicate was composed of four plants). Different letters on the graph bars indicate significant differences based on Tukey's test at the 5% significance level.

Table 1

Features of the soybean *GmHub10* (*Glyma.19G008200*) and its interactor genes retrieved from the *Glycine max* Wm82.a2.v1 (BioProject: PRJNA19861) genome dataset from the Phytozome v.12 database.

Gene ID	Gene function annotations	Gene length	Chromosome	Chromosome location (START)	Chromosome location (END)	CDD domain search	HMMER prediction	NLS motif
<i>Glyma.19G008200</i> (<i>GmHub10</i>)	pollen tube growth; regulation of defense response	3623	Chr19	810694	814316	Tetratricopeptide repeat (pfam13424)	Tetratricopeptide repeat	yes
<i>Glyma.01G146600</i>	cGMP-dependent protein kinase; phosphoprotein phosphatase; PKG II	8587	Chr01	48181319	48189905	Serine/threonine phosphatases (cd00143), protein kinases (cl21453), and effector domain of the CAP family of transcription factors (cd00038)	Protein phosphatase 2C	no
<i>Glyma.01G218300</i>	Deoxynucleotidyltransferase terminal-interacting protein 2	3627	Chr01	54838494	54842120	Fcf2 pre-rRNA processing (pfam08698)	Fcf2 pre-rRNA processing	yes
<i>Glyma.03G007200</i>	Zinc finger (Ran-binding) protein	4694	Chr03	651721	656414	Zn-finger in Ran-binding protein and others (pfam00641)	Zn-finger in Ran-binding protein and others	no
<i>Glyma.09G194200</i>	cGMP-dependent protein kinase; phosphoprotein phosphatase; PKG II	9799	Chr09	41851899	41861697	Serine/threonine phosphatases (cd00143), protein kinases (cl21453), and effector domain of the CAP family of transcription factors (cd00038)	Protein phosphatase 2C	No
<i>Glyma.11G024900</i>	Deoxynucleotidyltransferase terminal-interacting protein 2	3317	Chr11	1761162	1764478	Fcf2 pre-rRNA processing (pfam08698)	Fcf2 pre-rRNA processing	yes
<i>Glyma.14G125600</i>	Deoxynucleotidyltransferase terminal-interacting protein 2	5695	Chr14	19904641	19910335	Fcf2 pre-rRNA processing (pfam08698)	Fcf2 pre-rRNA processing	yes
<i>Glyma.14G125900</i>	Deoxynucleotidyltransferase terminal-interacting protein 2	1353	Chr14	19926735	19928087	Fcf2 pre-rRNA processing (pfam08698)	Fcf2 pre-rRNA processing	yes
<i>Glyma.19G118900</i>	Zinc finger (Ran-binding) protein	6233	Chr19	37651114	37657346	Zn-finger in Ran-binding protein and others (pfam00641)	Zn-finger in Ran-binding protein and others	no
<i>Glyma.20G012700</i>	Early growth response protein-related; zinc finger protein 7	717	Chr20	1070336	1071052	No conserved domains	–	no
<i>Glyma.07G190600</i>	Anaphase-promoting complex subunit 4 (APC4)	10702	Chr7	35824136	35834837	Anaphase-promoting complex subunit 4 (pfam12894 and pfam12896) and WD40 repeat (COG2319)	Anaphase-promoting complex, cyclosome, subunit 4	no

main inflorescence (Fig. 4A) and abortion of some flower buds (Fig. 4B) compared with wild-type control plants. In addition, a low seed germination rate and lower root yield were also observed for this mutant line. To assess whether the interaction of Minc00344 and Mj-NULG1a effectors with soybean *GmHub10* protein may be associated with an increase in plant susceptibility, the *AtHub10* mutant was inoculated with 250 *M. incognita* J2 and evaluated over time compared with wild-type and *AtEds1* lines (both used as susceptibility controls). The *AtHub10* mutant plants showed susceptibility levels (nematode penetration efficiency, post penetration development, and formation and morphology of the galls) similar to those of wild-type and *AtEds1* control plants. In addition, *AtHub10* mutant plants showed a higher number of eggs, J2, and galls per gram of roots compared to the wild-type plants, while no differences were observed compared to *AtEds1* mutant plants (Fig. 4C to E). However, no difference in the number of eggs, J2, and galls per plant was observed between the plant lines evaluated, since *AtHub10* plants produce lower root yields. In this way, *AtHub10* mutant plants showed similarities in the NRF values with the wild-type and *AtEds1* mutant plants (Fig. 4F). These data showed that *AtHub10* mutant plants were as susceptible as wild-type and *AtEds1* lines to the nematode, and the knockout of the *AtHub10* gene has serious consequences for both the plant and indirectly for the nematode's infectious cycle.

4. Discussion

PPNs are a large group of phytopathogens that, during plant-pathogen interactions, secrete effector proteins to promote parasitism by disrupting the plant defense response and modulate host developmental pathways (Vieira and Gleason 2019). This arsenal of nematode effectors when secreted in plant cells targets important host molecular components and can interfere in complex pathways to promote parasitism in different plant species (Quentin et al., 2013). In contrast, beyond preformed defenses, plants present another arsenal of molecules associated with basal defense responses (Vieira and de Almeida Engler 2017; Sato et al., 2019; Cabral et al., 2020). Initially, the root damage caused by nematode infection produces molecules that act as damage-associated molecular patterns (DAMPs) that, consequently, activate pattern-triggered immunity (PTI). In addition, pathogen-associated molecular patterns (PAMPs) or, specifically in the case of nematode infections, nematode-associated molecular patterns (NAMPs) enhancing the basal plant defense (PAMPs triggered immunity). The second level of plant defense responses against nematode infection is related to effector-triggered immunity (ETI) (Holbein et al., 2016). In consequence, numerous effectors act suppressing the signaling or activation of the PTI or ETI (Manosalva et al., 2015; Zhao et al., 2019).

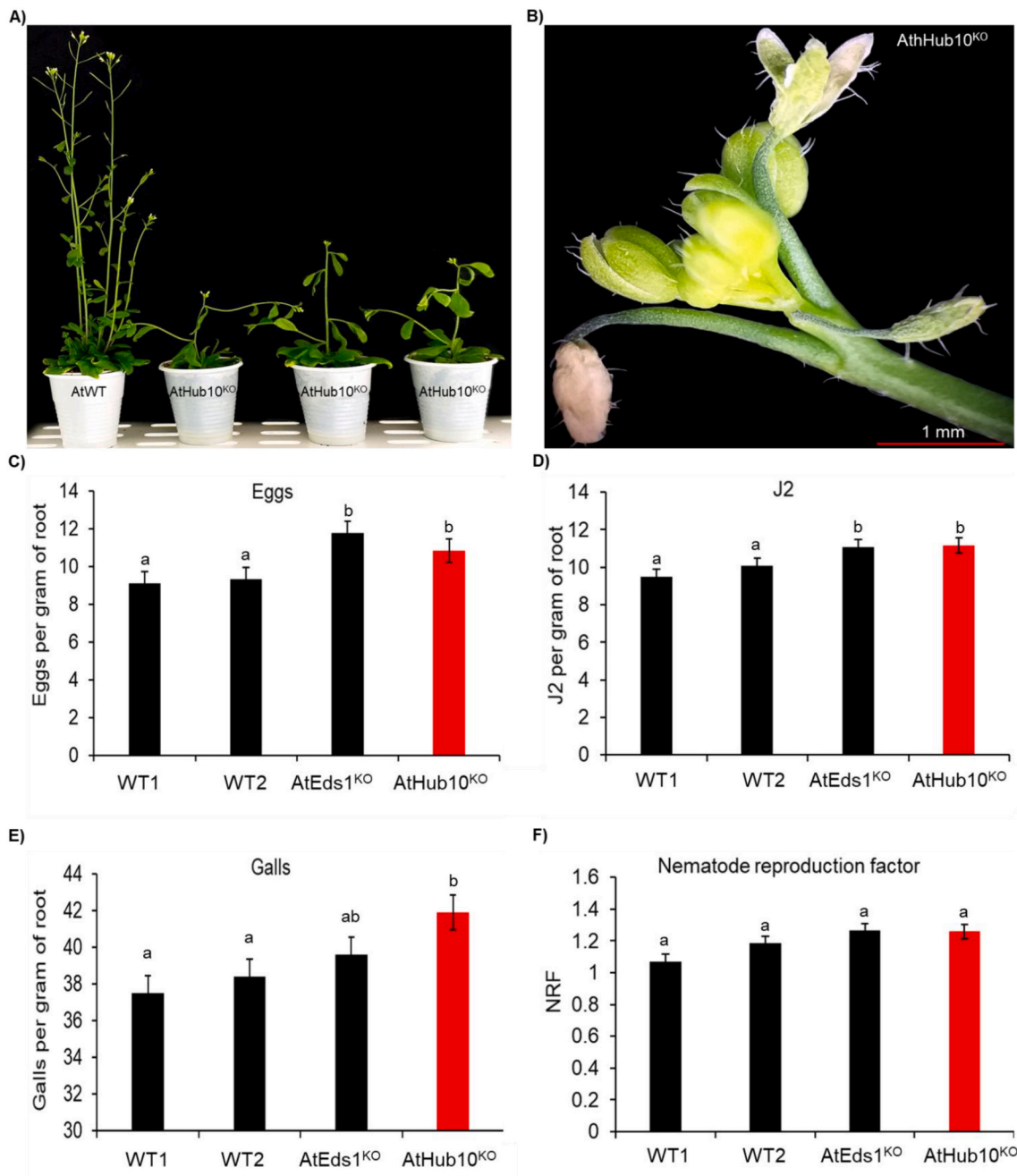


Fig. 4. Plant phenotype and susceptibility to the *M. incognita* race 3 of the *A. thaliana* mutant (T-DNA insertion) line to the *AtHub10* (*AT3G27960*) gene (SALK mutant: SALK_142719) compared to the Col-0 ecotype (wild-type; WT) and null mutant line to the *Enhanced disease susceptibility 1* (*Eds1*; *AT3G48090*; SALK mutant: SALK_034340) gene. *A. thaliana* mutant lines were obtained from Arabidopsis Biological Resource Center (ABRC; Columbus OH, 43210, USA). *A. thaliana* mutant line to the *AtHub10* gene (*AtHub10^{KO}*) showing (A) abnormal formation of the nodes and axillary flowers of the main inflorescence compared to wild-type control plants, and (B) abortion of some flower buds. (C) Number of eggs per gram of roots, (D) number of *M. incognita* J2 per gram of roots, (E) number of galls per plant, and (F) nematode reproduction factor (NRF) in *A. thaliana* wild-type (*AtWT1* and *AtWT2*), *A. thaliana* *Eds1* mutant (*AtEds1^{KO}*), and *A. thaliana* *Hub10* mutant (*AtHub10^{KO}*) at 40 days post-inoculation. Error bars represent confidence intervals corresponding to three technical replicates (E, F, and H) or corresponding to each plant evaluated (G), while each treatment was composed of 15 to 20 plants. Different letters on the graph bars indicate significant differences based on Tukey's test at 5% significance level.

The RKN complex is a major crop pathogen worldwide, and the limited range of available control agents or resistant cultivars has significantly limited the efficiency of its control and management (Seo and Kim 2014; Bernard et al., 2017). There are sedentary endoparasitic nematodes that spend most of their life cycle inside the roots and feed on giant cells, going from mobile preparasitic J2 until the females' oviposition. This infection cycle lasts approximately 30 to 60 days and is only possible if there is a compatible plant-nematode interaction (Ali et al.,

2018). The host plant and RKN fight a real battle based on defense, attack, and counterattack. The defense response suppression and reprogramming of plant cells by nematode effectors are essential for penetration, giant cell induction, feeding, and oviposition (egg masses) (Abad et al., 2003). After genome sequencing from *M. incognita* and *M. javanica* (Abad et al., 2008; Blanc-Mathieu et al., 2017), several effector proteins were already identified and characterized, but information about their function after secretion in the host plant or the way

they work is still poorly understood (Bellafiore et al., 2008; Lin et al., 2013; Rutter et al., 2014; Mejias et al., 2019).

In this study, the effectors Minc00344 and Mj-NULG1a were characterized slightly more regarding their involvement in the host plant parasitism by *M. incognita*. Both effectors showed low sequence identity and distant phylogenetic relationships, suggesting at the first moment a distinct mode of action after delivery in the host plant. Rutter et al. (2014) showed that Minc00344 were expressed in SvG and upregulated at 3 to 14 dpi, suggesting their involvement in the formation of giant cells and as putative avirulence proteins, respectively. In contrast, Lin et al. (2013) showed that the *Mj-NULG1a* gene was upregulated in dorsal gland cells at the beginning of parasitism, while the Mj-NULG1a protein was colocalized in the nuclei of giant cells. In addition, the downregulation of this effector using the RNAi strategy attenuated the parasitic ability of *M. javanica*, while *A. thaliana* overexpressing *Mj-NULG1a* was considered more susceptible (Lin et al., 2013). At the second moment supported by our data, similarly to *Minc00344* gene, the *Mj-NULG1a* gene is more expressed in J2 parasitic stages and acts in the nuclei of giant cells during nematode parasitism (Lin et al., 2013). This previous data can suggest that both these two effectors from different *Meloidogyne* species can act in a similar time during parasitism targeting the Hub10 protein. In addition, previous work by Mukhtar et al. (2011), Consortium (2011), and Wessling et al. (2014) has shown that different and diverse pathogen effectors can target the same hub protein. Curiously, our data showed that both these effector proteins interact specifically with the soybean GmHub10 protein, and the functional disruption of the GmHub10 protein during parasitism is a hypothesis in this study. To support this hypothesis, several interactions between nematode effectors and host plant proteins have already been characterized and have been associated with the suppression of host resistance (Goverse and Smant 2014; Mejias et al., 2019). For example, Hamamouch et al. (2012) showed that the *Heterodera schachtii* 30C02 effector protein interacts with a β -1,3-endoglucanase (*At4G16260*) enzyme of *A. thaliana* to suppress host defense responses and promote parasitism. Similarly, Zhao et al. (2019) showed that the *M. incognita* MiMIF-2 effector protein interacts with *A. thaliana* annexins (AnnAt1 and AnnAt4) to suppress plant immunity and facilitate nematode parasitism. In addition, Davies et al. (2015) showed that the *M. chitwoodi* Mc1194 effector protein interacts with a papain-like cysteine protease responsive to dehydration (RD21A), while *A. thaliana rd21-1* mutants were hypersusceptible to this nematode. In another example, the *M. javanica* MjTTL5 effector protein interacts with an *A. thaliana* ferredoxin:thioredoxin reductase catalytic subunit (*AtFTRc*) and suppresses plant immunity by activating the host reactive oxygen species-scavenging system (Lin et al., 2016). In our study, the Minc00344 and Mj-NULG1a effectors and GmHub10 protein interactions have been suggested to be associated with increased susceptibility of the *A. thaliana* AtHub10 mutant to *M. incognita*. Interestingly, AtHub10 has also been shown to be the target of interaction with other effector proteins of different pathogens (Mukhtar et al., 2011; Wessling et al., 2014). Kong and Hanley-Bowdoin (2002) showed that the geminivirus replication-associated (AL1) protein also interacts with a kinesin-like protein (*AT5G65460*; KIN14B) to prevent infected cells from undergoing mitosis. Accordingly, both nematodes and geminiviruses need to manipulate the host plant cell cycle to promote parasitism. Since *Minc0344* is upregulated in the J2 and J2/J3 stages, similar to the *Mj-NULG1a* effector gene, which is upregulated at the beginning of parasitism (Lin et al., 2013), it is suggested that the nematode inactivates Hub10 proteins for two reasons: i) prevent indirect Hub10 disturbance from activating the plant's defense responses, and ii) disrupt the cell cycle and make the plant cell more suitable for parasitism. Given these findings, it is possible to highlight the importance of AtHub10 or GmHub10 proteins in the activation of the host immune system, and the local disruption of these Hub10 proteins can be essential to modulate the plant cell cycle and promote plant infection.

Based on gene expression profile in resistant and susceptible soybean plants, our data indicate consistently that *GmHub10* mRNA expression

profile was not induced or modulated by the *M. incognita* infection, in both susceptible or resistant soybean plants. However, it is clearly observed that the *GmHub10* gene expression profile was significantly higher in the nematode-resistant plants (PI595099 genotype) in both mock or inoculated conditions. In this first moment, the higher GmHub10 protein accumulation can be suggested as associated with higher resistance to nematodes. Coincidentally, at 3 days after inoculation, the same time when the greatest accumulation of GmHub10 protein was observed in resistant plants, it is the exact time in which the nematode *M. incognita* or *M. javanica* has already come into contact with the root of the host plant, migrated until the candidate cell to be parasitized, and started to modulation the cell cycle and the defense mechanisms of these cells in order to make a favorable environment for him to be able to parasitism. However, in resistant plants where there is a high accumulation of GmHub10 protein, it is suggested that even using effectors to modulate or inactivate GmHub10 protein activity, this nematode counter-defense mechanism is not sufficient to prevent the activation of the plant's immune system and/or enough to modulate the cell cycle in a way that is desirable to the nematode parasitism.

The GmHub10 protein is previously known as essential to plant growth and development, and also closely related (direct or indirect involved) to the cell cycle mechanism (Reddy and Day 2001; Li et al., 2019). In this same sense, it is previously known that nematodes modulate the plant cell cycle and/or defense response to create the feeding sites and successfully parasitize the plant (de Almeida Engler et al., 2015; de Souza Junior et al., 2017). Our data showed that the constitutive knockdown of the *Hub10* gene resulted in aberrant plants; consequently, and notably, these mutant plants are not a good host plant to *M. incognita*. It is important to remember that these nematodes modulate the Hub10 protein activity in site- and cell-specific of adult plants. In view of this, we can suggest that the constitutive knockout of Hub10 is not desirable for either plant development or the nematode infection.

In addition, although *M. incognita* or *M. javanica* have several hundred effector proteins, our data showed that the downregulation of any of these evaluated effectors is considered highly relevant for impairing nematode parasitism. Thus, the loss of function of only one of these effectors during parasitism may be enough to fail to achieve full suppression of the host defense.

5. Conclusion

Several features of the Minc00344 and Mj-NULG1a effectors were highlighted in this study, and their substantial importance for successful plant infection was suggested. Next, protein-protein interaction assays showed that Minc00344 and Mj-NULG1a effectors interact in both *in vitro* and *in vivo* systems with soybean GmHub10 protein. The interactions between nematode effectors and soybean GmHub10 protein were suggested as a mechanism associated with an increase of plant susceptibility to nematode infection by the disruption of GmHub10 protein activity. In addition, considering the high conservation of these effectors in other *Meloidogyne* species, the downregulation of these target genes in different RKN species could be assessed. Finally, our findings showed that these two nematode effectors and the soybean *GmHub10* gene could be powerful targets for developing NBTs based on RNA interference and gene upregulation, respectively, for RKN control in important crops.

Authors' contributions

MFGS was the leading researcher for all the work and provided intellectual input and financial support. MFGS, RRF, and RAGM selected the soybean proteins, nematode effectors, and planned the experiments. RRF, JFA, MGS, and SNTD performed the soybean hub genes amplification, cloning, sequencing, and gene sequence analysis. MFB performed *in silico* analysis, gene expression assays and wrote the

manuscript. MFB, RAGM, TPR, and VSM performed the production of *M. incognita* inoculum, plant inoculation, and evaluated all bioassays. RAGM, RNL, and BPM performed the protein-protein interaction assays. MFSG, RRF, EVSA, MCMS, FV, and DF provided intellectual input. All authors read and approved the final version.

Consent for publication or ethics approval and consent to participate

Not applicable.

Funding

RAGM is grateful to CAPES by the doctoral research fellowship, and MFB is grateful to CNPq by the postdoctoral research fellowship (PDJ 150936/2018-4) and DF was supported by a visiting scientist grant from the Science without Borders program (project N° 400328/2012-7). This work was supported by grants from CAPES, CNPq, FAP-DF, INCT PlantStress Biotech, and EMBRAPA, Part of this research was funded by Agropolis Fondation (Montpellier, France) under the reference ID 1102-004 and by IRD-CNPq bilateral project.

Declaration of competing interest

All authors declare that the research was carried out in the absence of any commercial or financial relationships that could be construed as a potential conflict of interest.

Acknowledgments

We are grateful to EMBRAPA, UCB, CAPES, CNPq, INCT PlantStress Biotech, and FAP-DF for scientific and financial support. We also thank Bruna Medeiros Pereira for kindly providing the initial inoculum of *M. incognita* race 3.

Appendix A. Supplementary data

Supplementary data to this article can be found online at <https://doi.org/10.1016/j.exppara.2021.108153>.

References

- Abad, P., Favery, B., Rosso, M.N., Castagnone-Sereno, P., 2003. Root-knot nematode parasitism and host response: molecular basis of a sophisticated interaction. *Mol. Plant Pathol.* 4 (4), 217–224. <https://doi.org/10.1046/j.1364-3703.2003.00170.x>.
- Abad, P., Gouzy, J., Aury, J.-M., Castagnone-Sereno, P., Danchin, E.G.J., Deleury, E., Perfus-Barbeoch, L., Anthouard, V., Artiguenave, F., Blok, V.C., Caillaud, M.-C., Coutinho, P.M., Dasilva, C., De Luca, F., Deau, F., Esquibet, M., Flutre, T., Goldstone, J.V., Hamamouch, N., Hewezi, T., Jaillon, O., Jubin, C., Leonetti, P., Magliano, M., Maier, T.R., Markov, G.V., McVeigh, P., Pesole, G., Poulain, J., Robinson-Rechavi, M., Sallet, E., Séguens, B., Steinbach, D., Tytgat, T., Ugarte, E., van Ghelder, C., Veronico, P., Baum, T.J., Blaxter, M., Blevé-Zacheo, T., Davis, E.L., Ewbank, J.J., Favery, B., Grenier, E., Henrissat, B., Jones, J.T., Laudet, V., Maule, A. G., Quesneville, H., Rosso, M.-N., Schiex, T., Smant, G., Weissenbach, J., Wincker, P., 2008. Genome sequence of the metazoan plant-parasitic nematode *Meloidogyne incognita*. *Nat. Biotechnol.* 26, 909. <https://doi.org/10.1038/nbt.1482>.
- Abdelkhalek, A., Ismail, I.A., Dessoky, E.S., El-Hallous, E.I., Hafez, E., 2019. A tomato kinesin-like protein is associated with *Tobacco mosaic virus* infection. *Biotechnol. Biotechnol. Equip.* 33 (1), 1424–1433. <https://doi.org/10.1080/13102818.2019.1673207>.
- Abel, S., Bürstenbinder, K., Müller, J., 2013. The emerging function of IQD proteins as scaffolds in cellular signaling and trafficking. *Plant Signal. Behav.* 8 (6), e24369. <https://doi.org/10.4161/psb.24369>.
- Ali, M.A., Anjam, M.S., Nawaz, M.A., Lam, H.-M., Chung, G., 2018. Signal transduction in plant-nematode interactions. *Int. J. Mol. Sci.* 19 (6), 1648. <https://doi.org/10.3390/ijms19061648>.
- Basso, M., Arraes, F.B.M., Grossi-de-Sa, M., Moreira, V.J.V., Alves-Ferreira, M., Grossi-de-Sa, M.F., 2020a. Insights into genetic and molecular elements for transgenic crop development. *Front. Plant Sci.* 11, 509. <https://doi.org/10.3389/fpls.2020.00509>.
- Basso, M.F., Ferreira, P.C.G., Kobayashi, A.K., Harmon, F.G., Nepomuceno, A.L., Molinari, H.B.C., Grossi-de-Sa, M.F., 2019. MicroRNAs and new biotechnological tools for its modulation and improving stress tolerance in plants. *Plant Biotechnology Journal.* <https://doi.org/10.1111/pbi.13116>.
- Basso, M.F., Lourenço-Tessutti, I.T., Mendes, R.A.G., Pinto, C.E.M., Bournaud, C., Gillet, F.-X., Togawa, R.C., de Macedo, L.L.P., de Almeida Engler, J., Grossi-de-Sa, M. F., 2020b. *MiDa16-like* and *MiSkn1-like* gene families are reliable targets to develop biotechnological tools for the control and management of *Meloidogyne incognita*. *Sci. Rep.* 10 (1), 6991. <https://doi.org/10.1038/s41598-020-63968-8>.
- Bellaïf, S., Shen, Z., Rosso, M.N., Abad, P., Shih, P., Briggs, S.P., 2008. Direct identification of the *Meloidogyne incognita* secretome reveals proteins with host cell reprogramming potential. *PLoS Pathog.* 4 (10), e1000192. <https://doi.org/10.1371/journal.ppat.1000192>.
- Beneventi, M.A., da Silva Jr., O.B., de Sá, M.E.L., Firmino, A.A.P., de Amorim, R.M.S., Albuquerque, E.V.S., da Silva, M.C.M., da Silva, J.P., Campos, M.A., Lopes, M.J.C., Togawa, R.C., Pappas Jr., G.J., Grossi-de-Sa, M.F., 2013. Transcription profile of soybean-root-knot nematode interaction reveals a key role of phytohormones in the resistance reaction. *BMC Genom.* 14. <https://doi.org/10.1186/1471-2164-14-322>, 322–322.
- Bernard, G.C., Egnin, M., Bonsi, C., 2017. The impact of plant-parasitic nematodes on agriculture and methods of control. *Nematology - Concepts, Diagnosis and Control.* <https://doi.org/10.5772/intechopen.68958>.
- Blanc-Mathieu, R., Perfus-Barbeoch, L., Aury, J.-M., da Rocha, M., Gouzy, J., Sallet, E., Martin-Jimenez, C., Bailly-Bechet, M., Castagnone-Sereno, P., Flot, J.-F., Kozłowski, D.K., Cazareth, J., Couloux, A., da Silva, C., Guy, J., Kim-Jo, Y.-J., Rancurel, C., Schiex, T., Abad, P., Wincker, P., Danchin, E.G.J., 2017. Hybridization and polyploidy enable genomic plasticity without sex in the most devastating plant-parasitic nematodes. *PLoS Genet.* 13 (6), e1006777. <https://doi.org/10.1371/journal.pgen.1006777>.
- Bournaud, C., Gillet, F.-X., Murad, A.M., Bresso, E., Albuquerque, E.V.S., Grossi-de-Sá, M. F., 2018. *Meloidogyne incognita* PASSE-MURAILLE (MiPM) gene encodes a cell-penetrating protein that interacts with the CSN5 subunit of the COP9 signalosome. *Front. Plant Sci.* 9 (904). <https://doi.org/10.3389/fpls.2018.00904>.
- Burstenbinder, K., Savchenko, T., Müller, J., Adamson, A.W., Stamm, G., Kwong, R., Zipp, B.J., Dinesh, D.C., Abel, S., 2013. Arabidopsis calmodulin-binding protein IQ67-domain 1 localizes to microtubules and interacts with kinesin light chain-related protein-1. *J. Biol. Chem.* 288 (3), 1871–1882. <https://doi.org/10.1074/jbc.M112.396200>.
- Bybd, D.W., Kirkpatrick, T., Barker, K.R., 1983. An improved technique for clearing and staining plant tissues for detection of nematodes. *J. Nematol.* 15 (1), 142–143.
- Cabral, D., Banora, M.Y., Antonino, J.D., Rodiuc, N., Vieira, P., Coelho, R.R., Chevalier, C., Eekhout, T., Engler, G., de Veylder, L., Grossi-de-Sa, M.F., de Almeida Engler, J., 2020. The plant WEE1 kinase is involved in checkpoint control activation in nematode-induced galls. *New Phytol.* 225 (1), 430–447. <https://doi.org/10.1111/nph.16185>.
- Calil, I.P., Quadros, I.P.S., Araújo, T.C., Duarte, C.E.M., Gouveia-Mageste, B.C., Silva, J.C. F., Brustolini, O.J.B., Teixeira, R.M., Oliveira, C.N., Milagres, R.W.M.M., Martins, G. S., Chory, J., Reis, P.A.B., Machado, J.P.B., Fontes, E.P.B., 2018. A WW domain-containing protein forms immune nuclear bodies against begomoviruses. *Mol. Plant* 11 (12), 1449–1465. <https://doi.org/10.1016/j.molp.2018.09.009>.
- Carneiro, R.G., Mazzafera, P., Ferraz, L.C.C.B., Muraoka, T., Trivelin, P.C.O., 2002. Uptake and translocation of nitrogen, phosphorus and calcium in soybean infected with *Meloidogyne incognita* and *M. javanica*. *Fitopatologia Brasileira* 27, 141–150.
- Castagnone-Sereno, P., Danchin, E.G.J., Perfus-Barbeoch, L., Abad, P., 2013. Diversity and evolution of Root-knot nematodes, genus *Meloidogyne*: new insights from the genomic Era. *Annu. Rev. Phytopathol.* 51 (1), 203–220. <https://doi.org/10.1146/annurev-phyto-082712-102300>.
- Castagnone-Sereno, P., Semblat, J.P., Castagnone, C., 2009. Modular architecture and evolution of the *map-1* gene family in the root-knot nematode *Meloidogyne incognita*. *Mol. Genet. Genom.* 282 (5), 547–554. <https://doi.org/10.1007/s00438-009-0487-x>.
- Consortium, A.I.M., 2011. Evidence for network evolution in an Arabidopsis interactome map. *Science* 333 (6042), 601–607. <https://doi.org/10.1126/science.1203877>.
- Cui, H., Gobbato, E., Kracher, B., Qiu, J., Bautor, J., Parker, J.E., 2017. A core function of EDS1 with PAD4 is to protect the salicylic acid defense sector in Arabidopsis immunity. *New Phytol.* 213 (4), 1802–1817. <https://doi.org/10.1111/nph.14302>.
- Danchin, E.G.J., Arguel, M.-J., Campan-Fournier, A., Perfus-Barbeoch, L., Magliano, M., Rosso, M.-N., da Rocha, M., da Silva, C., Nottet, N., Labadie, K., Guy, J., Artiguenave, F., Abad, P., 2013. Identification of novel target genes for safer and more specific control of Root-knot nematodes from a pan-genome mining. *PLoS Pathog.* 9 (10), e1003745. <https://doi.org/10.1371/journal.ppat.1003745>.
- Das, A.K., Cohen, P.W., Barford, D., 1998. The structure of the tetratricopeptide repeats of protein phosphatase 5: implications for TPR-mediated protein-protein interactions. *EMBO J.* 17 (5), 1192–1199. <https://doi.org/10.1093/emboj/17.5.1192>.
- Davies, L.J., Zhang, L., Elling, A.A., 2015. The *Arabidopsis thaliana* papain-like cysteine protease RD21 interacts with a root-knot nematode effector protein. *Nematology* 17 (6), 655–666. <https://doi.org/10.1163/15685411-00002897>.
- de Almeida Engler, J., Kyndt, T., Vieira, P., Van Cappel, E., Boudolf, V., Sanchez, V., Escobar, C., de Veylder, L., Engler, G., Abad, P., Gheysen, G., 2012. *CCS52* and *DELI* genes are key components of the endocycle in nematode-induced feeding sites. *Plant J.* 72 (2), 185–198. <https://doi.org/10.1111/j.1365-313X.2012.05054.x>.
- de Almeida Engler, J., Van Poucke, K., Karimi, M., de Groodt, R., Gheysen, G., Engler, G., Gheysen, G., 2004. Dynamic cytoskeleton rearrangements in giant cells and syncytia of nematode-infected roots. *Plant J.* 38 (1), 12–26. <https://doi.org/10.1111/j.1365-313X.2004.02019.x>.
- de Almeida Engler, J., Vieira, P., Rodiuc, N., Grossi de Sa, M.F., Engler, G., 2015. Chapter Four - the plant cell cycle machinery: Usurped and modulated by plant-parasitic nematodes. In: Escobar, C., Fenoll, C. (Eds.), *Advances in Botanical Research*, vol. 73. Academic Press, pp. 91–118. <https://doi.org/10.1016/bs.abra.2014.12.003>.

- roots of parasitism and its potential for molecular mimicry. *PLoS One* 8 (6), e67377. <https://doi.org/10.1371/journal.pone.0067377>.
- Shukla, N., Yadav, R., Kaur, P., Rasmussen, S., Goel, S., Agarwal, M., Jagannath, A., Gupta, R., Kumar, A., 2018. Transcriptome analysis of root-knot nematode (*Meloidogyne incognita*)-infected tomato (*Solanum lycopersicum*) roots reveals complex gene expression profiles and metabolic networks of both host and nematode during susceptible and resistance responses. *Mol. Plant Pathol.* 19 (3), 615–633. <https://doi.org/10.1111/mpp.12547>.
- Silva, M.S., Arraes, F.B.M., Campos, M.A., Grossi-de-Sa, M., Fernandez, D., Cândido, E.S., Cardoso, M.H., Franco, O.L., Grossi-de-Sa, M.F., 2018. Review: potential biotechnological assets related to plant immunity modulation applicable in engineering disease-resistant crops. *Plant Sci.* 270, 72–84. <https://doi.org/10.1016/j.plantsci.2018.02.013>.
- Szklarczyk, D., Gable, A.L., Lyon, D., Junge, A., Wyder, S., Huerta-Cepas, J., Simonovic, M., Doncheva, N.T., Morris, J.H., Bork, P., Jensen, L.J., Mering, C.V., 2019. STRING v11: protein-protein association networks with increased coverage, supporting functional discovery in genome-wide experimental datasets. *Nucleic Acids Res.* 47 (D1), D607–D613. <https://doi.org/10.1093/nar/gky1131>.
- Tomalova, I., Iachia, C., Mulet, K., Castagnone-Sereno, P., 2012. The map-1 gene family in Root-knot nematodes, *Meloidogyne* spp.: a set of taxonomically restricted genes specific to clonal species. *PLoS One* 7 (6), e38656. <https://doi.org/10.1371/journal.pone.0038656>.
- Triantaphyllou, A., Hirschmann, H., 1960. Post infection development of *Meloidogyne incognita* Chitwood 1949 (Nematoda-Heteroderidae). In: *Annales de l'Institut Phytopathologique Benaki*, vol. 1, pp. 1–11.
- Trudgill, D.L., Blok, V.C., 2001. Apomictic, polyphagous root-knot nematodes: exceptionally successful and damaging biotrophic root pathogens. *Annu. Rev. Phytopathol.* 39, 53–77. <https://doi.org/10.1146/annurev.phyto.39.1.53>.
- USDA, 2020. World Agricultural Production. United State Department of Agriculture - Circular series WAP, 2-2020.
- Vieira, P., de Almeida Engler, J., 2017. Plant cyclin-dependent kinase inhibitors of the KRP family: Potent inhibitors of Root-knot nematode feeding sites in plant roots. *Front. Plant Sci.* 8, 1514. <https://doi.org/10.3389/fpls.2017.01514>.
- Vieira, P., Gleason, C., 2019. Plant-parasitic nematode effectors - insights into their diversity and new tools for their identification. *Curr. Opin. Plant Biol.* 50, 37–43. <https://doi.org/10.1016/j.pbi.2019.02.007>.
- Wessling, R., Epple, P., Altmann, S., He, Y., Yang, L., Henz, S.R., McDonald, N., Wiley, K., Bader, K.C., Glasser, C., Mukhtar, M.S., Haigis, S., Ghamsari, L., Stephens, A.E., Ecker, J.R., Vidal, M., Jones, J.D., Mayer, K.F., Ver Loren van Themaat, E., Weigel, D., Schulze-Lefert, P., Dangl, J.L., Panstruga, R., Braun, P., 2014. Convergent targeting of a common host protein-network by pathogen effectors from three kingdoms of life. *Cell Host Microbe* 16 (3), 364–375. <https://doi.org/10.1016/j.chom.2014.08.004>.
- Wheeler, T.J., Eddy, S.R., 2013. *NHMMER: DNA homology search with profile HMMs*. *Bioinformatics (Oxford, England)* 29 (19), 2487–2489. <https://doi.org/10.1093/bioinformatics/btt403>.
- Windham, G.L., Williams, W.P., 1987. Host suitability of commercial corn hybrids to *Meloidogyne arenaria* and *M. incognita*. *J. Nematol.* 19 (Annals 1), 13–16.
- Xie, J., Li, S., Mo, C., Wang, G., Xiao, X., Xiao, Y., 2016. A novel *Meloidogyne incognita* effector Misp12 suppresses plant defense response at latter stages of nematode parasitism. *Front. Plant Sci.* 7 <https://doi.org/10.3389/fpls.2016.00964>, 964–964.
- Xue, B., Hamamouch, N., Li, C., Huang, G., Hussey, R.S., Baum, T.J., Davis, E.L., 2013. The 8D05 parasitism gene of *Meloidogyne incognita* is required for successful infection of host roots. *Phytopathology* 103 (2), 175–181. <https://doi.org/10.1094/phyto-07-12-0173-r>.
- Zhao, J., Li, L., Liu, Q., Liu, P., Li, S., Yang, D., Chen, Y., Pagnotta, S., Favery, B., Abad, P., Jian, H., 2019. A MIF-like effector suppresses plant immunity and facilitates nematode parasitism by interacting with plant annexins. *J. Exp. Bot.* 70 (20), 5943–5958. <https://doi.org/10.1093/jxb/erz348>.